Progression characteristics of ellipsoid zone loss in macular telangiectasia type 2.

Daniel Pauleikhoff[1,2], Roberto Bonelli[3,4], Adam M Dubis[5,6], Frederic Gunnemann[1], Kai Rothaus[1], Peter Charbel Issa[7], Tjebo FC Heeren[8,6,5], Tunde Peto[9,10], Traci E Clemons[11], Emily Y Chew[12], Alan C Bird[13], Ferenc B Sallo[5, 6, 14] and the MacTel Study Group.

[1]Department of Ophthalmology, St. Franziskus Hospital, Münster, Germany
[2]Department of Ophthalmology, University of Duisburg-Essen, Germany
[3]Population Health and Immunity, Walter and Eliza Hall Institute of Medical Research, Parkville, Victoria, Australia
[4]Department of Medical Biology, University of Melbourne, Melbourne, Australia
[5]UCL Institute of Ophthalmology, London, United Kingdom
[6]Moorfields Eye Hospital, London, United Kingdom, Department of Research and Development
[7]Oxford Eye Hospital, Oxford University Hospitals NHS Foundation Trust, and Nuffield Laboratory of Ophthalmology, Department of Clinical Neurosciences, University of Oxford, Oxford, United Kingdom
[8]Department of Ophthalmology, University Hospital Bonn, Germany
[9]Queen's University Belfast Faculty of Medicine, Health and Life Sciences, Belfast, UK
[10]NIHR Biomedical Research Center for Ophthalmology, at Moorfields Eye Hospital NHS Foundation Trust and UCL Institute of Ophthalmology, London, UK
[11]The Emmes Corporation, Rockville, Maryland, USA
[12]National Eye Institute, National Institutes of Health, Bethesda, Maryland, USA
[13]Moorfields Eye Hospital, London, United Kingdom, Inherited Eye Disease
[14]Department of Ophthalmology, University of Lausanne, Hôpital Ophtalmique Jules-Gonin, Fondation Asile des aveugles, Switzerland

[*] Correspondence should be directed to:

Ferenc B Sallo MD, PhD
Department of Research and Development
Moorfields Eye Hospital NHS Foundation Trust
162 City Road, London, EC1V 2PD, UK
Phone: +44 207 566 2815
Fax: +44 207 608 6925
Email: f.sallo@ucl.ac.uk

ABSTRACT

Purpose:

To investigate the progression characteristics of ellipsoid zone (EZ) loss in eyes with macular telangiectasia type 2 (MacTel) as reflected by area and linear measurements, and their relevance for visual acuity.

Methods:

Participants were selected from the MacTel Study cohort. Linear and area measurements of EZ loss were performed in SD-OCT volume scans. Progression characteristics and correlations between linear and area measurements were analyzed using linear mixed effects models.

Results:

A total of 134 eyes of 70 patients were included (85 eyes with follow-up, mean 4.7 years, range 1.4-8 years). EZ loss significantly progressed at a mean annual increment of 0.057mm^2 ($p=0.005$). The progression rate was non-linear and interacted significantly with initial EZ lesion size indicating an exponential growth before reaching a plateau. There was a strong heterogeneity in area sizes between fellow eyes. EZ break length had a significant linear effect on EZ break area ($b=1.06$, $p<0.001$) and could predict it. The location of the EZ break had a significant impact on visual acuity.

Conclusions:

EZ loss in MacTel has a non-linear progression characteristic and its rate depends on area size at baseline, which must be taken into account at sample selection in clinical trials. Our results show a good correlation of linear and area measures of EZ loss and a segregation of BCVA by EZ location, which may help routine clinical practice.

Key Words:

Macular Telangiectasia Type 2, MacTel, Ellipsoid zone, En face image, OCT

INTRODUCTION

According to our current understanding, Macular Telangiectasia Type 2 (MacTel) is a bilateral, neurodegenerative disease, with proposed initial dysfunction and eventual loss of Müller cells resulting in a characteristic clinical phenotype. (Powner et al. 2010; Charbel Issa et al. 2013; Powner et al. 2013) Typical structural changes include vascular abnormalities seen in color fundus photographs, fundus autofluorescence images, and fluorescein angiography (demonstrating dilated, blunted and right-angle veins, telangiectatic deep capillaries), a loss of retinal transparency with a corresponding hyper-reflectivity best visible in blue-light reflectance images and a redistribution of macular pigment (MP) as recorded by dual-wavelength autofluorescence. (Gass 1968; Gass & Oyakawa 1982; Gass & Blodi 1993; Charbel Issa et al. 2008; Esposti et al. 2012; Charbel Issa et al. 2013; Sallo et al. 2018) Morphological changes observable in SD-OCT images are also highly characteristic of this disease. (Gaudric et al. 2006) These include a thinning of the central retina, low-reflective spaces ('cavities') in the inner and outer retina, and a focal loss of the ellipsoid zone (EZ, also known as a break in the IS/OS layer) which typically starts temporal to the foveal center, progresses to involve the foveal center, later extending also to the nasal macula. (Sallo et al. 2015) This loss of the EZ has been demonstrated to correlate closely with focal retinal function loss as measured by mesopic microperimetry, by electrophysiology (multifocal ERG) and - once it affects the foveal center – by loss of best-corrected visual acuity. (Sallo et al. 2012a; Sallo et al. 2012b; Mukherjee et al. 2017; Heeren et al. 2018; Okada et al. 2018; Peto et al. 2018)

Although slowly progressive, MacTel may lead to a bilateral loss of central vision and as yet there is no therapy available. It is therefore of considerable importance to provide outcome measures for following disease severity and progression that are precise, accurate and reproducible for potential clinical trials and also such that are practical and informative for clinicians.

Previous studies demonstrated that area measurements of a break in the EZ may be used as a surrogate parameter for the severity and progression of the disease as it corresponds closely with function loss (Sallo et al. 2012a; Sallo et al. 2012b; Chew et al. 2015; Mukherjee et al. 2017; Sallo et al. 2018). This endpoint was explored in a phase 2 clinical trial of an intravitreal encapsulated device producing ciliary neurotrophic factor (CNTF) in MacTel. (Mukherjee et al. 2017)

Our aim was to investigate the progression characteristics (dynamics) of the EZ break in participants enrolled in a natural history study of MacTel in order to provide data for planning future treatment trials.

METHODS

All participants in this study were selected from the cohort of the Natural History Observation (NHO) and Registry (NHOR) Studies of Macular Telangiectasia type 2 (MacTel). Details of the MacTel NHO/R Studies are described elsewhere. (Clemons et al. 2010; Clemons et al. 2013) The study protocol adhered to the tenets of the Declaration of Helsinki and was approved by the local institutional ethics committee. Written informed consent was obtained from each participant after explanation of the nature of the study.

Imaging

Patients underwent annual examinations including best-corrected visual acuity (BCVA) measurement and SD-OCT imaging. Details of the standard operation procedures have been published previously. (Clemons et al. 2010)

OCT imaging was performed on Heidelberg Spectralis devices (OCT or HRA+OCT; Heidelberg Engineering, Heidelberg, Germany) using the following parameters: in high-resolution mode, a volume scan centered on the fovea, covering an area of at least 15 degrees horizontally and 10 degrees vertically, was acquired at a maximal B-scan interval of 30µm (at least 97 scans/volume).

Measurements

Within the volume scan, the B-scan traversing the foveal center was selected, and the length of the EZ break along this B-scan was measured using the caliper tool of the native Heidelberg Eye Explorer software of Heidelberg Spectralis devices (Heyex, version 6.0.13.0, Heidelberg Engineering), expressed in mm. The volume scans were segmented using the "all layers" automated segmentation provided by Heyex, with the option of manual correction. In particular, the photoreceptor segmentation line "PR1" was reviewed and corrected manually as necessary. This line defines the ellipsoid zone (see Figure 1.). The option of 'transverse' imaging within the 3D view panel of Heyex allowed for *en face (transverse)* visualization of the EZ layer (along the plane of the retina). The PR1 line was set as the base reference for the *en face* image, the offset distance and slab thickness were set to 0, resulting in a slab of a single pixel thickness, centered on the EZ. The color table for the OCT image was set to "White on Black" resulting in a darker area for EZ loss. The "draw region" tool of Heyex was then used to delineate the darker area of the suspected EZ loss in an overlay superimposed in the *en face* panel. In a next step, the position of boundary markers of the overlay was compared in each B-scan with the apparent edges of the break. In both linear and area measurements, only a clear EZ loss was accepted as a break, an attenuation of the EZ signal alone was not considered a break. If the lines of the overlay did not co-locate with the edges of EZ loss, the correct position of EZ loss was marked manually within the *en face* image. Based on the manual markers, a new overlay was drawn within the *en face* image. This procedure was repeated until a satisfactory correspondence between the EZ loss boundaries in the B-scans and the overlay was achieved. Usually, no more than two iterations were necessary. In the en-face images, the break area was expressed in mm^2 by Heyex (see Figure 1B). As axial length information was not available, the default setting for retinal magnification ("medium axial length", Gullstrand 1911) was used for all measurements.

Functional correlates of the EZ break

To investigate the functional significance of EZ break location relative to the foveal center, eyes were grouped accordingly (see Figure 2.) and the BCVA of eyes in groups 1 (no EZ break), 2 (EZ break not involving the foveal center) and 3 (EZ break involving also the foveal center) were compared.

Statistical analyses

The progression of EZ loss was analyzed using linear mixed effects modeling. Each model included two random intercepts, one for each participant, and one for each eye of each participant. A random intercept was used for each eye to account for within-eye correlation. Heterogeneity of EZ loss area within fellow eyes of patients was tested through inclusion of random terms and Intra-Class Correlation (ICC).

To assess the magnitude of the prediction error we compared the median absolute deviation (MdAD) which measures the amount of deviation from the median EZ break area in the sample with the median absolute error (MdAE) which measures the deviation of predicted EZ break areas from their respective real areas.

Functional correlates of EZ break topographic location relative to the foveal center was tested using a linear mixed model that included only a random intercept for each eye. Due to the small sample size, we were only able to include a fixed effect for time.

Diagnostic residuals plots were created to test the assumptions of the models. Residual relationships between break length and EZ loss area were tested using Pearson's residuals.

Given the hypothesis generation goal of this investigation, a p-value of < 0.05 was accepted as statistically significant. Analyses were conducted using R v3.3.2 available under a GNU GPL v2 license (R Development Core Team, www.r-project.org).

RESULTS

A total of 134 eyes of 70 patients were included (mean age at baseline: 62.5 years, SD 9.4 years, range 34.7-84.5 years; 32 males, 38 females). The mean follow-up period was 4.7 years, SD=1.4 years, range 1.4-8 years, n=85 eyes of 43 patients with follow up. Mean BCVA at baseline was logMAR 0.28 (range 1.16 to -0.06 to 1.16, SD=0.23, approximate Snellen equivalents: mean=20/40, range 20/18 – 20/300, n=85 eyes). One eye was excluded due to the presence of a macular hole.

EZ break progression characteristics - linear and area measurements

Mean EZ loss area at baseline was 0.54 mm^2 (SD=0.64 mm^2, range: 0-2.67 mm^2). Mean EZ break linear loss at baseline was 0.57 mm (SD=0.57 mm, range: 0-2.41 mm). EZ loss significantly progressed at a mean annual increment of 0.057mm^2 (p=0.005).

To determine whether all EZ loss across patients had the same progression rate between patients and between fellow eyes we tested whether the inclusion of specific random slopes in the model significantly increase the model fitness. The inclusion of a random slope for progression in each patient was significant compared to the non-inclusion (p<0.001) indicating the presence of heterogeneity in growth rate between subjects. The inclusion of an additional random slope for each eye also significantly increased the model fitness (p<0.001) and made the random slope for each subject non-essential (p=0.99) highlighting that also fellow eyes do not progress at the same rate. The same result was obtained for the inclusion/exclusion of random intercepts to test heterogeneity between area sizes in patients and eyes, indicating that also in area sizes there is a strong heterogeneity even between fellow eyes. Nonetheless, the intra class correlation (ICC) measure (0.63, CI: 0.51-0.72) indicates a moderate symmetry between fellow eyes.

Given the above results, we noted that the progression rate of each subject was really dependent on the size of the baseline break area, indicating a strong, non-linear progression. For this reason, we fitted a linear mixed model with only a random intercept for each eye and took into account differences in patients' progression by including an interaction between time and the tertiles of baseline EZ loss area respectively (0-0.37), (0.37-0.95) and (0.95-2.67) respectively. The study time effect (defined as numbers of years from the baseline visit) in the first group of initial break area was significant (b=0.056, P<0.001) indicating an average increment among eyes in this group of 0.056 mm^2 per year. In the second group, the time effect was larger than in previous group (b=0.126 P<0.001) indicating a faster progression (0.126 mm^2 per year) for eyes that already reached a break area between 0.37 and 0.95 mm^2. In the last group, progression was still faster than in the first group but smaller than the second group (b=0.102, P<0.001) indicating a plateau effect. We did not find a significant association between baseline area size and the subjects' gender or age.

The result from the previous model highlighted a very strong non-linearity in the progression rate that is unique for each eye, depending on the EZ loss area already reached. To illustrate the characteristics of the non-linear growth better, we present estimated relationship between time and area size stratified by different initial area sizes in Figure 3. From this image we note how the growth rate increases in the second group to then slow down in the third group.

Correlation of linear and area measurements

To test whether there is a significant correlation between break length and break area, we included break length in a linear mixed effect model that ignored time and initial area size. EZ Break length appeared to have a significant linear effect on EZ loss area (b=1.06, p<0.001). This result indicates that for each 1 mm increment in break length, there is ~1 mm^2 increment in EZ break area.

We also tested whether there was a non-linear relationship between break length and EZ loss area. The results of this analysis are shown in Supplementary Figure 1. From this figure, we can see that there is no relationship left to be explained between EZ break area and break length that was not already explained by the linear association in the model.

Given the linearity in the association between EZ break length and area, we tested if the former could be used as a clinical surrogate to predict the latter. To do this, we used cross-validation and predicted each subject's EZ break area at different time points by estimating the model on all other subjects. Comparing the observed EZ break area and predicted EZ break area, we obtained an MdAD of 0.56mm^2 and an MdAE of 0.15mm^2. These results indicate that the error of predicting the area by using length was almost four times lower than the natural variability of EZ break area within the sample. Moreover, correlation between predicted and real break areas was 0.89. These results highlight the power and reliability of predicting break areas using break lengths.

To understand the prediction tool better, we compared the relationship between real break areas and predicted ones with the identity line in Figure 4. From this figure, we note how our prediction pattern (blue line) tends to be below the identity line (red line) for values higher than 1.5mm^2 in break area size. This indicates that large EZ loss area predictions tend to be slightly underestimated using break length.

Differences in central visual function by EZ break location

The functional correlates of the EZ break by topographic location were assessed by investigating the differences in BCVA across groups 1-3 (group 1: no EZ break, group 2: EZ break not involving the foveal center, and group 3: EZ break also at the foveal center) in 80 eyes, observed 2 times (160 data points, also see Figure 5).

We did not observe differences between groups 1 and 2 (p= 0.537). However, a significant difference was observed between groups 1 and 3. Eyes in group 3 had on average a 0.31 increase in logMAR scale compared to group 1 (p= 3.58E-08). The difference between groups 2 and 3 was also significant (p=2.51E-11). Size of break area also influenced visual acuity by a 0.06 increase in logMAR scale for each mm^2 (p=0.017).

DISCUSSION

In the present study we consistently found an overall progression of the EZ loss but with high variability. The mean annual progression rate of EZ break area in our present sample was 0.057 mm^2. In previous studies, Sallo et al found an annual progression rate of 0.14mm^2, (SE = 0.040), (Sallo et al. 2012b) whereas Heeren et al. found approximately 0.08mm^2, (SD = 0.014), (Heeren et al. 2018).

It is noted that Sallo et al. analyzed OCT scans acquired on a different device (Topcon 3D-OCT1000) and used a different technique for delineating and measuring EZ breaks, which may explain the differences in EZ measurements. Calibration for true retinal image size (taking into consideration the axial length and refractive power of respective individual eye) was not performed in any of these studies, however in view of the sample sizes, a significant effect is not expected.

These differences may however also be due to the different inclusion criteria used in the three studies. Sallo et al. (2012b) included only eyes that already showed EZ loss at baseline whereas in the sample analyzed by Heeren et al., eyes were included regardless of the presence or absence of EZ loss at baseline which is similar to the current study.

We found direct evidence that the rate of increase in EZ break area is not linear. We observed an exponential growth of EZ break area before reaching a plateau. This needs to be taken into account in controlled therapeutic trials. The plateau effect may be explained by the lesion size approaching the full extent of the “MacTel area”. Based on comparative clinical and histological observations, (Powner et al. 2010; Powner et al. 2013) Fruttiger et al. proposed the term 'MacTel area' (personal communication), defined as the outer boundary of an area with abnormally increased reflectivity to blue light, and noted that most abnormalities associated with the disease appear located within this oval (or circular) boundary centered on the fovea, defined initially by blue light reflectance imaging. Although considerable individual variability is detectable in the size and ratio of the vertical and horizontal diameters of this area from case to case, in a sample of 65 eyes, a mean size of approximately 3064µm horizontally and 2338µm vertically and a V/H ratio of 0.77 was found. (Sallo et al. 2018) Reaching the full extent of this area may be hypothesized to represent the ‘end-stage’ also for the EZ lesion size and our current data do indicate a trend towards such an expected maximum value of the EZ break area. Nonetheless, in our sample we only had a small number of data points in this area size range and previous studies were also largely limited to subjects with early disease. Further investigations are indicated for establishing the growth rates of very large lesions and lesions that are affected with the end-stage subretinal neovascularization associated with MacTel.

Although our data show a moderate symmetry in the growth rate of incident EZ breaks between fellow eyes, nonetheless, a high variability was present. Highly variable progression rates are also known from other 'atrophic' macular diseases, including geographic atrophy in Age-Related Macular Degeneration. (Holz et al. 2007) Part of this asymmetry could be due to the non-linear nature of the EZ break area progression rate. If one eye has a break and the fellow eye doesn’t, the primary incident break will grow over time, along the characteristics shown in Figure 3. Although the initial growth rate appears nearly linear, by the time the fellow eye also develops a break, the primary incident break may already have reached an area size at which we start seeing an exponential growth rate. At this point, the secondary break will grow at a linear rate whereas the growth rate of the primary break will be exponential. Despite this variability, in a larger sample it will be possible to differentiate

'slow' and 'fast' progressors, which will open the door to an analysis of the relative significance of genetic, metabolic, and environmental factors in the progression of the disease (Scerri et al. 2017), thereby providing prognostic advice to affected patients, suggesting possible treatment strategies as well as aiding patient selection for future clinical trials.

The functional relevance and utility of EZ loss area measurements for following disease progression in MacTel have been demonstrated previously and our data are in accordance with previous findings (see Figure 5). (Sallo et al. 2012a; Sallo et al. 2012b; Mukherjee et al. 2017) The results of the present study demonstrate that linear measurements of EZ loss in a horizontal foveal B-scan - that can easily be acquired routinely in a clinical setting - can also be considered representative of the severity of the disease and appear to be useful parameters for describing the extent of photoreceptor loss (or abnormality) in MacTel eyes. Admittedly, EZ loss area measurements reflect pathological changes more accurately and are preferable for use in treatment trials. For clinical use however, in view of constraints in terms of time, effort and the limited availability of software tools, a linear measurement in a single foveal B-scan would be more practical. One limitation of this method may be that for lesions 1.5mm^2 or larger in area, the linear measurement tends to underestimate the area size, although the differences are small.

The incidence of EZ loss and the extension of the EZ loss to the foveal center are landmark events in MacTel. The former has a functional relevance documented using a psychophysical method with reasonable repeatability (microperimetry) and as the break grows, it causes increasing visual disability due to a pre-fixational scotoma. The latter event directly affects central vision as the fovea is involved. (Peto et al. 2018) Both events are possible to document reliably using OCT imaging - an objective, structural method. Our data further demonstrate the impact of the EZ break and its location on visual acuity (see Figure 2). Another possible major event in MacTel is the incidence of subretinal neovascular proliferation (SRNV). (Peto et al. 2018) This appears to be a secondary complication of the disease and may occur at any point during the evolution of the disease. The prevalence of SRNV was estimated to 12.1% in one study investigating a sample of 1244 affected MacTel probands. (Leung et al. 2018) SRNV may threaten central vision directly and responds to anti-vascular endothelial growth factor (vEGF) therapy, whereas the basic neuro-degenerative disease process does not. (Kupitz et al. 2015)

We acknowledge, that both linear and area measurements of EZ loss have limitations. Occasionally, linear measurements may not reflect area size if the lesion is in a position not traversed by the foveal scan, or of a supero-inferiorly oblong shape. Some boundaries of the EZ break may be indistinct, variability of signal-to-noise ratios as well as scan directionality may be sources of bias, such that care should be taken for consistency in delineating lesions when analyzing images captured over time. Fluctuations in area size at consecutive scans may be attributable to measurement error, although biological causes are also conceivable and change in EZ break area may not always be unidirectional.

Establishing the position of the foveal center accurately in advanced MacTel may also be challenging, as the photoreceptor matrix, the distribution of luteal pigment and the foveal contour are all likely to be affected by the disease. Although the shape of the foveal avascular zone may also be affected, it is advisable to include this vascular cue in determining the position of the foveal center, especially in more advanced disease. Keeping historical images is a major advantage. It should also be kept in mind that whenever it is attempted to constrain a process continuous in time and a lesion in lateral extent into

distinct and artificial categorical subdivisions, some cases will be borderline or not fit the system. (Zeffren et al. 1990)

In conclusion, the demonstrated non-linear characteristics of EZ loss progression need to be taken into account both at patient selection and when assessing the validity of conclusions drawn from controlled therapeutic trials. The close correlation between linear and area measurements of EZ loss we found in our sample may provide clinicians with a simple tool for assessing disease severity.

ACKNOWLEDGEMENTS

Acknowledgement: Many thanks are due Ms Wirtz-Kirchberg for her great efforts in analyzing the SD-OCT scans and en-face images.

Financial support: The authors wish to thank the Lowy Medical Research Institute (LMRI) for providing funding for this study. R.B. was supported by the Melbourne International Research Scholarship as well as by Victoria State Government Operational Infrastructure Support and Australian Government NHMRC IRIISS funding. PCI is supported by National Institute for Health Research (NIHR) Oxford Biomedical Research Centre (BRC), Oxford, UK. AMD is supported by the NIHR Biomedical Research Centre at Moorfields Eye Hospital and UCL Institute of Ophthalmology.

Proprietary interest: Pauleikhoff D: none, Bonelli R: none, Dubis AM: none, Gunnemann F: none, Rothaus K: none, Charbel Issa P: none, Heeren TFC: none, Peto T: none, Clemons TE: none, Chew EY: none, Bird AC: none, Sallo F: none.

REFERENCES

Charbel Issa P, TT Berendschot, G Staurenghi, FG Holz & HP Scholl (2008): Confocal blue reflectance imaging in type 2 idiopathic macular telangiectasia. Invest Ophthalmol Vis Sci **49**: 1172-1177.

Charbel Issa P, MC Gillies, EY Chew, AC Bird, TF Heeren, T Peto, FG Holz & HP Scholl (2013): Macular telangiectasia type 2. Prog Retin Eye Res **34**: 49-77.

Chew EY, TE Clemons, T Peto, FB Sallo, A Ingerman, W Tao, L Singerman, SD Schwartz, NS Peachey & AC Bird (2015): Ciliary neurotrophic factor for macular telangiectasia type 2: results from a phase 1 safety trial. Am J Ophthalmol **159**: 659-666 e651.

Clemons TE, MC Gillies, EY Chew, AC Bird, T Peto, MJ Figueroa & MW Harrington (2010): Baseline characteristics of participants in the natural history study of macular telangiectasia (MacTel) MacTel Project Report No. 2. Ophthalmic Epidemiol **17**: 66-73.

Clemons TE, MC Gillies, EY Chew, AC Bird, T Peto, JJ Wang, P Mitchell, WD Ramdas & JR Vingerling (2013): Medical characteristics of patients with macular telangiectasia type 2 (MacTel Type 2) MacTel project report no. 3. Ophthalmic Epidemiol **20**: 109-113.

Esposti SD, C Egan, C Bunce, JD Moreland, AC Bird & AG Robson (2012): Macular Pigment Parameters in Patients with Macular Telangiectasia (MacTel) and Normal Subjects: Implications of a Novel Analysis. Invest Ophthalmol Vis Sci **53**: 6568-6575.

Gass JD (1968): A fluorescein angiographic study of macular dysfunction secondary to retinal vascular disease. V. Retinal telangiectasis. Arch Ophthalmol **80**: 592-605.

Gass JD & BA Blodi (1993): Idiopathic juxtafoveolar retinal telangiectasis. Update of classification and follow-up study. Ophthalmology **100**: 1536-1546.

Gass JD & RT Oyakawa (1982): Idiopathic juxtafoveolar retinal telangiectasis. Arch Ophthalmol **100**: 769-780.

Gaudric A, G Ducos de Lahitte, SY Cohen, P Massin & B Haouchine (2006): Optical coherence tomography in group 2A idiopathic juxtafoveolar retinal telangiectasis. Arch Ophthalmol **124**: 1410-1419.

Gullstrand A (1911): Methoden der Dioptrik des Auges des Menschen.

Heeren TFC, D Kitka, D Florea, TE Clemons, EY Chew, AC Bird, D Pauleikhoff, P Charbel Issa, FG Holz & T Peto (2018): Longitudinal Correlation of Ellipsoid Zone Loss and Functional Loss in Macular Telangiectasia Type 2. Retina **38 Suppl 1**: S20-S26.

Holz FG, A Bindewald-Wittich, M Fleckenstein, J Dreyhaupt, HP Scholl & S Schmitz-Valckenberg (2007): Progression of geographic atrophy and impact of fundus autofluorescence patterns in age-related macular degeneration. Am J Ophthalmol **143**: 463-472.

Kupitz EH, TF Heeren, FG Holz & P Charbel Issa (2015): Poor Long-Term Outcome of Anti-Vascular Endothelial Growth Factor Therapy in Nonproliferative Macular Telangiectasia Type 2. Retina **35**: 2619-2626.

Leung I, FB Sallo, R Bonelli, TE Clemons, D Pauleikhoff, EY Chew, AC Bird, T Peto & G MacTel Study (2018): Characteristics of Pigmented Lesions in Type 2 Idiopathic Macular Telangiectasia. Retina **38 Suppl 1**: S43-S50.

Mukherjee D, EM Lad, RR Vann, SJ Jaffe, TE Clemons, M Friedlander, EY Chew, GJ Jaffe & S Farsiu (2017): Correlation Between Macular Integrity Assessment and Optical Coherence Tomography Imaging of Ellipsoid Zone in Macular Telangiectasia Type 2. Invest Ophthalmol Vis Sci **58**: BIO291-BIO299.

Okada M, AG Robson, CA Egan, FB Sallo, SD Esposti, TFC Heeren, M Fruttiger & GE Holder (2018): Electrophysiological Characterization of Macular Telangiectasia Type 2 and Structure-Function Correlation. Retina **38 Suppl 1**: S33-S42.

Peto T, TFC Heeren, TE Clemons, FB Sallo, I Leung, EY Chew & AC Bird (2018): CORRELATION OF CLINICAL AND STRUCTURAL PROGRESSION WITH VISUAL ACUITY LOSS IN MACULAR TELANGIECTASIA TYPE 2: MacTel Project Report No. 6-The MacTel Research Group. Retina **38 Suppl 1**: S8-S13.

Powner MB, MC Gillies, M Tretiach, A Scott, RH Guymer, GS Hageman & M Fruttiger (2010): Perifoveal muller cell depletion in a case of macular telangiectasia type 2. Ophthalmology **117**: 2407-2416.

Powner MB, MC Gillies, M Zhu, K Vevis, AP Hunyor & M Fruttiger (2013): Loss of Muller's cells and photoreceptors in macular telangiectasia type 2. Ophthalmology **120**: 2344-2352.

Putnam NM, Hofer HJ, Doble N, Chen L, Carroll J, Williams DR (2005): The locus of fixation and the foveal cone mosaic. Journal of Vision 2005: 632-9

Sallo FB, I Leung, TE Clemons, T Peto, AC Bird & D Pauleikhoff (2015): Multimodal imaging in type 2 idiopathic macular telangiectasia. Retina **35**: 742-749.

Sallo FB, I Leung, M Zeimer, TE Clemons, AM Dubis, M Fruttiger, D Pauleikhoff, EY Chew, C Egan, T Peto & AC Bird (2018): Abnormal Retinal Reflectivity to Short-Wavelength Light in Type 2 Idiopathic Macular Telangiectasia. Retina **38 Suppl 1**: S79-S88.

Sallo FB, T Peto, C Egan, UE Wolf-Schnurrbusch, TE Clemons, MC Gillies, D Pauleikhoff, GS Rubin, EY Chew & AC Bird (2012a): "En face" OCT Imaging of the IS/OS Junction Line in Type 2 Idiopathic Macular Telangiectasia. Invest Ophthalmol Vis Sci **53**: 6145-6152.

Sallo FB, T Peto, C Egan, UE Wolf-Schnurrbusch, TE Clemons, MC Gillies, D Pauleikhoff, GS Rubin, EY Chew & AC Bird (2012b): The IS/OS junction layer in the natural history of type 2 idiopathic macular telangiectasia. Invest Ophthalmol Vis Sci **53**: 7889-7895.

Scerri TS, A Quaglieri, C Cai, J Zernant, N Matsunami, L Baird, L Scheppke, R Bonelli, LA Yannuzzi, M Friedlander, CA Egan, M Fruttiger, M Leppert, R Allikmets & M Bahlo (2017): Genome-wide analyses identify common variants associated with macular telangiectasia type 2. Nat Genet **49**: 559-567.

Wilk MA, AM Dubis, RF Cooper, P Summerfelt, A Dubra & J Carroll (2017): Assessing the spatial relationship between fixation and foveal specializations. Vision Res **132**: 53-61.

Zeffren BS, RA Applegate, A Bradley & WA van Heuven (1990): Retinal fixation point location in the foveal avascular zone. Invest Ophthalmol Vis Sci **31**: 2099-2105.

FIGURES

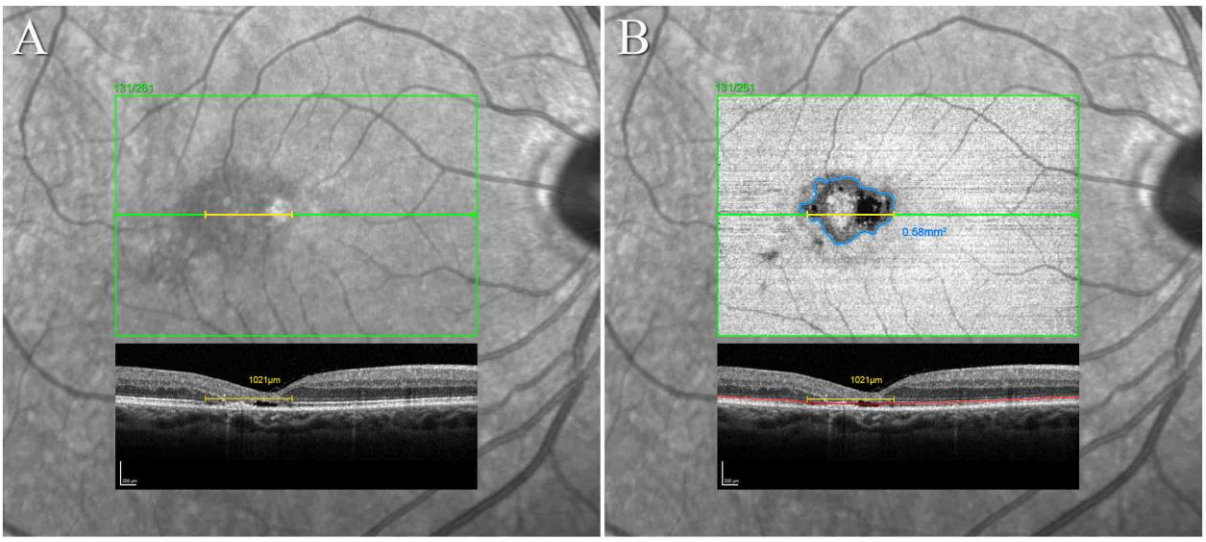

Figure 1. Linear and area measurements of the EZ break in SD-OCT volume scans.
A: Infrared SLO image with the position marker of the OCT volume scan and B-scan #131/261 traversing the foveal center superimposed. The caliper tool (yellow) was used to measure the lateral linear extent of the EZ break in this B-scan. **B:** The EZ en face image superimposed over the IR image in A. The EZ segmentation line is marked within the B-scan in red, the boundary of the break within the en face image of the EZ in blue. In this case, the EZ break also affects the foveal center. Only areas where the EZ was no longer apparent in the B-scan were accepted as a clear break. Mere attenuations of a signal still present were not accepted as a full EZ break (e.g. smaller dark areas infero-temporal to the main lesion in the en face image in B. These may however be early signals of a developing break).

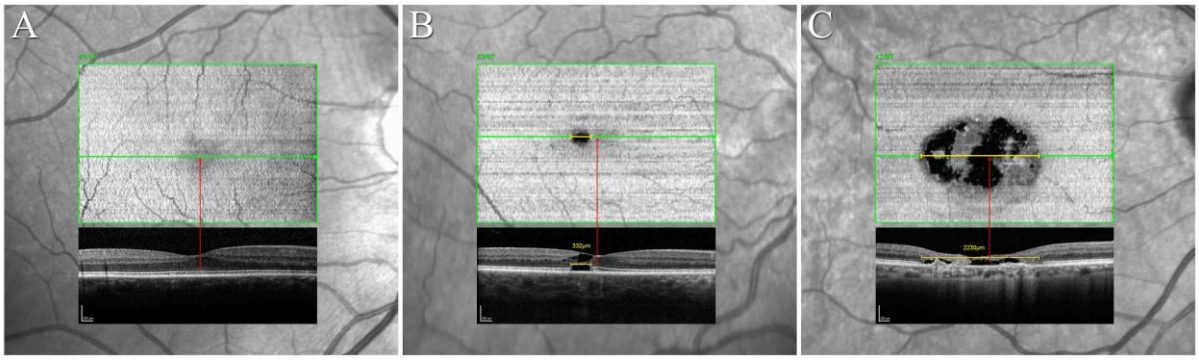

Figure 2. Topographic location of the EZ break relative to the foveal center.
The diagnosis in MacTel may be established based on any satisfactory combination of the characteristic signs of the disease: a redistribution of luteal pigment, the concomitant pattern of hyper-reflectivity to short-wavelength light, OCT low reflective spaces in the inner/outer retina without retinal thickening, OCT focal outer retinal atrophy, mostly with overall retinal thinning; vascular abnormalities (telangiectatic and/or dilated capillaries in the deep plexus, dilated, blunted or right angle veins), or perivascular pigment plaques predominantly in the mid-retina, all in the absence of extensive retinal thickening or cystoid macular edema. Given an established diagnosis, the incidence of an EZ break and when it reaches the foveal center are landmark events in MacTel.

Based on these two events, as reflected by OCT volume imaging, viewed either in B-scans or in transverse images of the Ellipsoid Zone, cases may be grouped: [A] Established MacTel disease, but no detectable EZ break. Contrast sensitivity, scotopic retinal sensitivity and reading speeds may be affected, BCVA and mesopic retinal sensitivity are preserved. [B] An EZ break is present but the nearest edge does not reach the foveal center. In these cases, mesopic microperimetry will demonstrate a scotoma co-locating with the area of the EZ break. BCVA is likely to be unaffected. [C] An EZ break is present and it also affects the foveal center. BCVA is likely to be affected. Subretinal neovascular proliferation (SRNV) or post-SRNV scarring is a secondary complication of MacTel, and may occur at any point in its natural history. SRNV may threaten central vision directly and responds to anti-vEGF therapy, whereas the basic disease process does not. At least a quick cursory en face glance is recommended in all eyes to exclude extreme cases e.g. with vertically oblong EZ breaks or major EZ breaks located largely outside the transfoveal scan. The functional relevance of the location of the EZ break is shown in Figure 5.

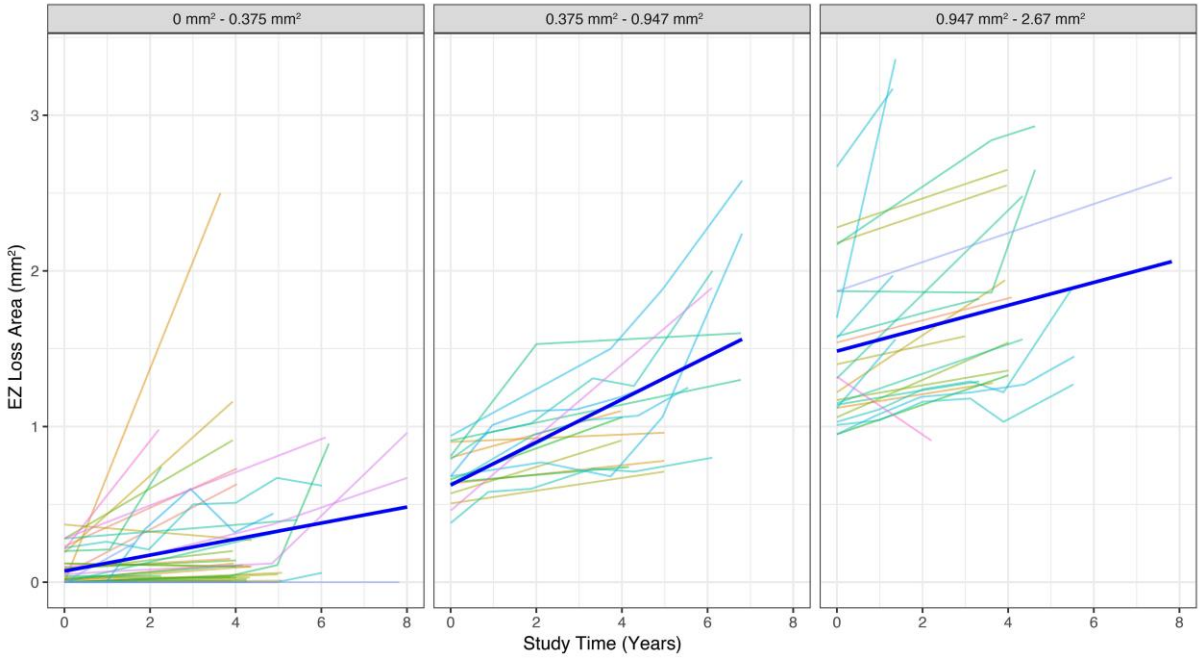

Figure 3. Observed and predicted growth curves at different initial break areas.
These line plots show the observed progression patterns of the EZ break area (thin colored lines) and the average predicted patterns form the model (bold blue lines) at different initial break area sizes. Note how the predicted progression pattern estimated by the model changes in each initial break area group (0-0.375mm^2, 0.375-0.947mm^2, and 0.947-2.67mm^2). This effect is indicating a non-linear progression of EZ break area that increases exponentially over time before reaching a plateau.

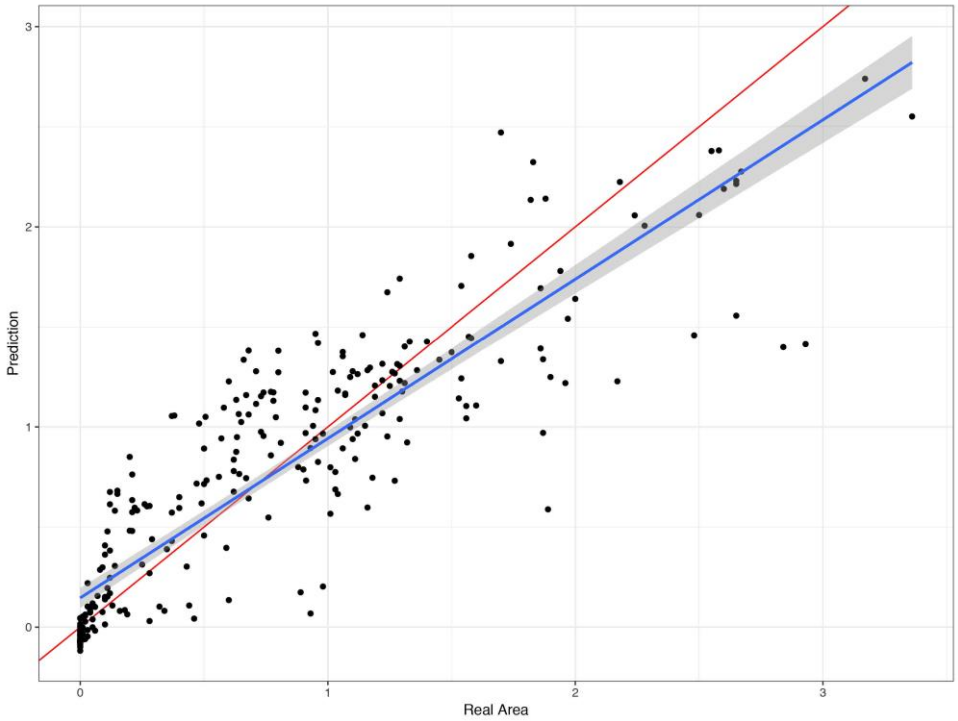

Figure 4: Relationship between real break areas and break areas predicted based on break length.

This figure demonstrates the relationship of predicted beak area values (based on break length) and the real observed break area. Each dot represents one such data pair, predicted size on the Y axis, measured size value on the X axis (both axes in mm^2). This figure also includes the estimated relationship between the predicted and the true areas (blue line) as well as the identity line (red line). Note how the relationship between linear and predicted areas overlaps with the identity line, indicating a strong predicting power.

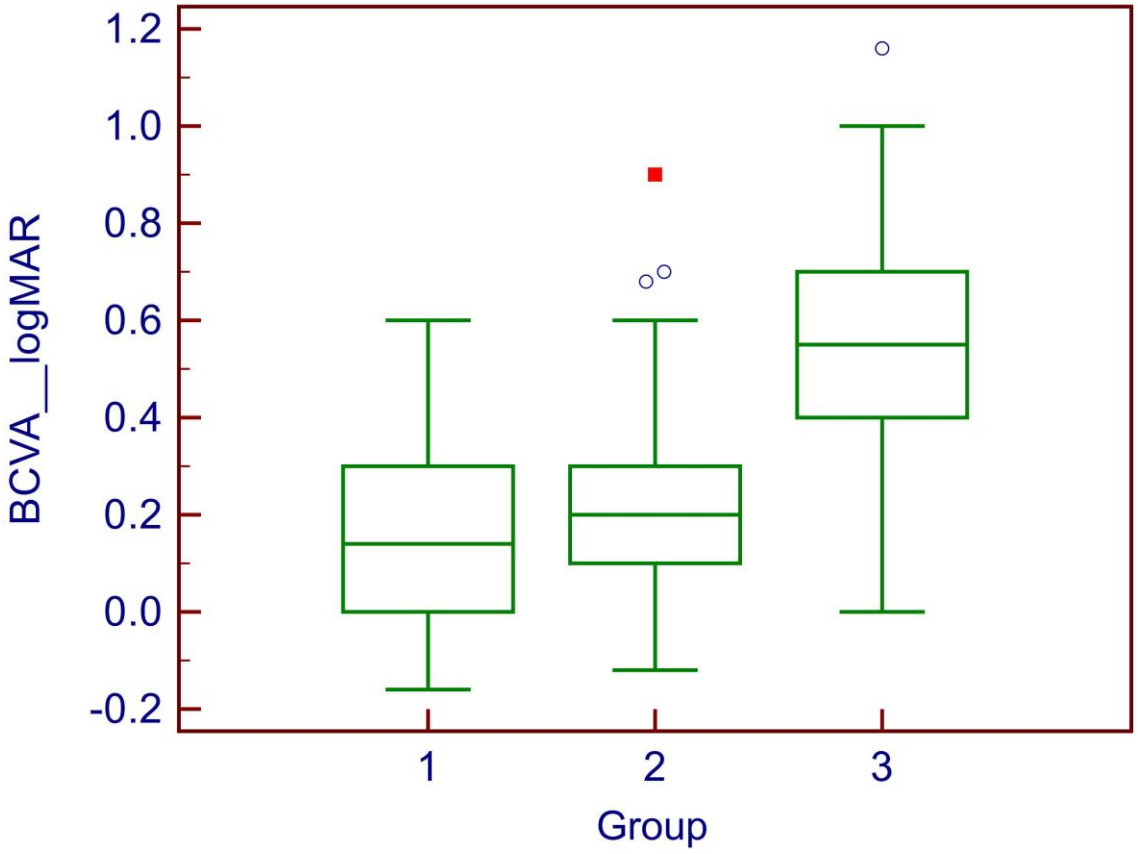

Figure 5: Distribution of BCVA values by location of the EZ break.

The differences in BCVA between groups 1 (no EZ break, n=24) and 2 (EZ break present but not involving the foveal center, n=93) were not statistically significant. In group 3 (n=43), two eyes had full vision. One explanation of good visual acuity despite the lesion reaching the foveal center in these outliers may be that fixation and the point of best acuity may not correspond exactly with the anatomical center of the fovea in all eyes.(Zeffren et al. 1990; Wilk et al. 2017; Putnam et al. 2005) Another possibility is that the absence of the EZ line may not indicate absence of structures that give rise to the line, but indicate distortion of alignment of these structures.

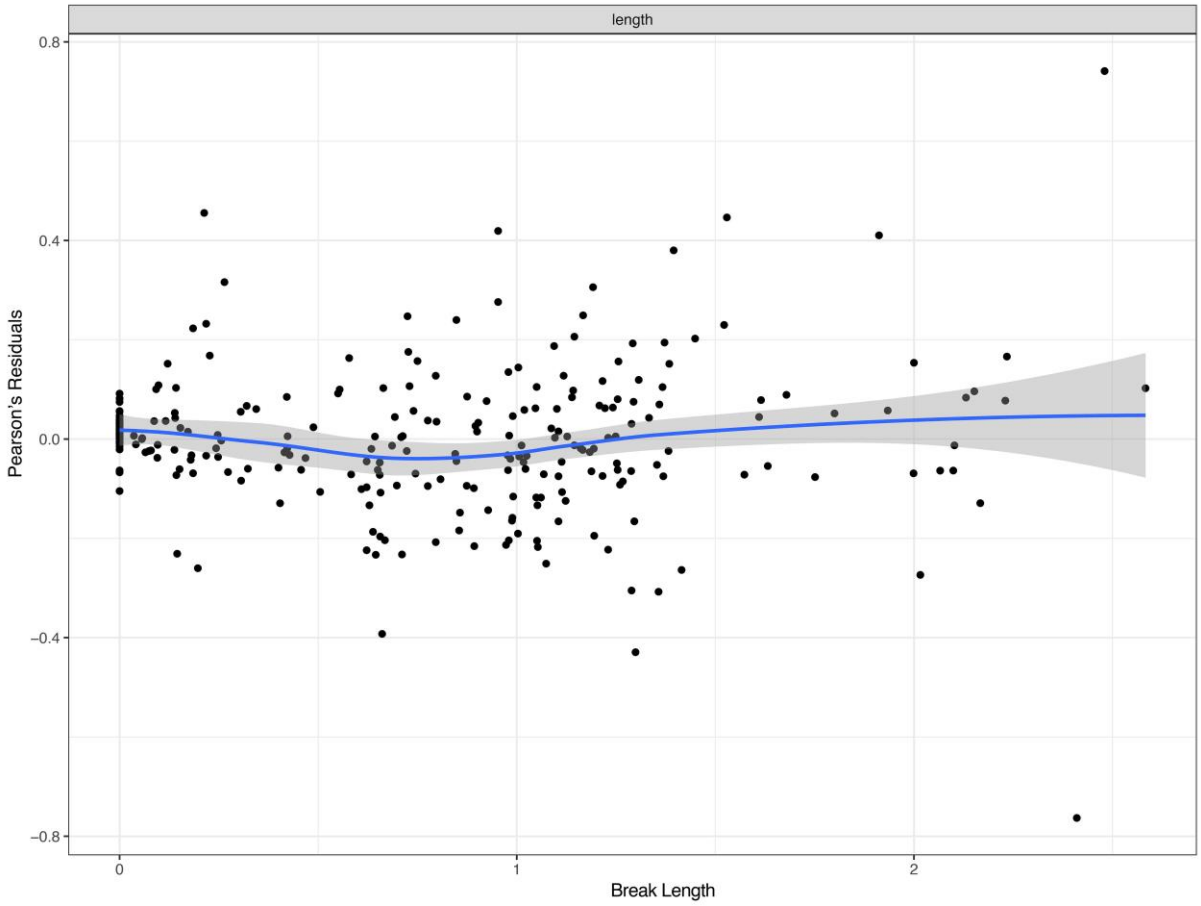

Online Supplementary Figure 1: EZ break area Pearson's residuals vs. EZ break length value. This figure demonstrates that there is no residual relationship between length and area to explain, the relationship is linear.

APPENDIX

Participating Principal Investigators and Centers in the MacTel Study:

Sophie Bakri, MD, Mayo Clinic, Rochester, MN, USA
Paul S Bernstein, MD, PhD, Moran Eye Center, University of Utah Health Care, Utah, UT, USA
Barbara Blodi, MD, University of Wisconsin School of Medicine and Public Health, Madison, WI, USA
Alexander Brucker, MD, Scheie Eye Institute, Philadelphia, PA, USA
Felicitas Bucher, MD, University of Freiburg Medical School Eye Center, Freiburg, Germany
Peter Charbel Issa, MD, Oxford Eye Hospital, Oxford, UK
Mina Chung, MD, University of Rochester, Rochester, NY, USA
Grant Comer, MD, University of Michigan Kellogg Eye Center, Ann Arbor, MI, USA
Ian Constable, MD, Lions Eye Institute, Nedlands, Western Australia, Australia
Michael Cooney,MD, Manhattan Eye Ear & Throat Hospital, New York, NY, USA
Diana Do, MD, Byers Eye Institute, Stanford University, Palo Alto, CA, USA
Jacque Duncan, MD, University of California San Francisco, San Francisco, CA, USA
Catherine Egan, MD, Moorfields Eye Hospital,London, UK
Michael J Elman, MD, Elman Retina Group PA, Baltimore, MD, USA
Amani Fawzi, MD, Northwestern University, Chicago, IL, USA
Martin Friedlander, MD, PhD, Scripps Research Institute, La Jolla, CA, USA
Alain Gaudric, MD, Hopital Lariboisiere, Paris, France
Mark C Gillies, MD, PhD, Save Sight Institute, Sydney, New South Wales, Australia
Roger Goldberg, MD, Bay Area Retina Associates, Walnut Creek, CA, USA
Joseph M Googe Jr., MD, Southeastern Retina Associates PC, Knoxville, TN, USA
Robyn Guymer, MD, Center for Eye Research, Melbourne, Victoria, Australia
Patrick Higgins, MD, Retina Center of New Jersey LLC, New Jersey, NJ, USA
Frank Holz, MD, University of Bonn, Bonn, Germany
Odette Houghton, MD, Mayo Clinic Scottsdale, AZ, USA
Carel B Hoyng, Prof., Radboud University Medical Center, Departments of Ophthalmology & Human Genetics, Nijmegen, Gelderland, The Netherlands
Jean-Pierre Hubschman, MD, Jules Stein Eye Institute, University of California, Los Angeles, CA, USA
Chirag Jhaveri, MD, Retina Research Center, Austin, TX, USA
Arshad Khanani,MD, Sierra Eye Associates, Reno, NV, USA
David Lally, MD, New England Retina Consultants PC, Springfield, MA, USA
Cecilia Lee, MD, University of Washington Eye Institute, Seattle, WA, USA
Michael Lee, MD, Retina Northwest, Portland, OR, USA
Joan W Miller, MD, Massachusetts Eye and Ear Infirmary Harvard Medical School, Boston, MA, USA
Daniel Miller,MD, Cincinnatti Eye Institute CEI Physicians PSC INC, Cincinnati, OH, USA
Joseph Moisseiev, MD, Goldschleger Eye Institute, Tel Hashomer, Ramat Gan, Israel
Robert Murphy, MD, The Retina Group of Washington, Fairfax, VA, USA
Raja Narayanan, MD, LV Prasad Eye Institute, Hyderabad, Telangana, India
Daniel Pauleikhoff, MD, PhD, St. Franziskus Hospital, Muenster, Germany
Sandeep Randhawa, MD, Associated Retinal Consultants PC Royal Oak, Royal Oak, MI, USA
Paul V Raphaelian, MD, Associated Retinal Consultants PC Grand Rapids, Grand Rapids, MI, USA
Ryan Rich, MD, Retina Consultants of Southern Colorado, Colorado Springs, CO, USA
Richard Rosen, MD, New York Eye and Ear Infirmary, New York, NY, USA
Philip Rosenfeld, MD, PhD, Bascom Palmer, Miami, FL, USA
Joke Ruys, MD, Oftalmologie, ZNA Middelheim, Antwerpen, Belgium
Jose-Alain Sahel, MD, PhD, Center Hopitalier National D'Optalmologie des Quinze-Vingts,Paris, France
Steven Schwartz, MD, Jules Stein Eye Institute UCLA, Los Angeles, CA, USA
Lawrence Singerman, MD, Retina Associates of Cleveland, Cleveland, OH, USA
Scott Sneed, MD, Associated Retinal Consultants PC Traverse City, Traverse City, MI, USA
Gisele Soubrane, MD, PhD, Clinique Ophtalmolgie de Creteil, Paris, France
Johannes R Vingerling, MD, PhD, Department of Ophthalmology Erasmus Medical Center Rotterdam, Rotterdam, The Netherlands
David Warrow, MD, Cumberland Valley Retina Consultants, Hagerstown, MD, USA

David Weinberg, MD, Medical College of Wisconsin Eye Institute, Milwaukee, WI, USA
Sebastian Wolf, MD, PhD, Department of Ophthalmology, Inselspital, University of Bern, Switzerland
Charles Wykoff, MD, PhD, Retina Consultants of Houston, Houston, TX, USA
Jiong Yan, MD, Emory Eye Center Emory University, Atlanta, GA, USA
Lawrence A Yannuzzi, MD, Vitreous retina macula consultants of New York, New York, NY, USA
Stanislav A Zhuk, MD, FACS, Retina Associates of New Orleans, Metairie, LA, USA